

**PARTONIC STRUCTURE AND DISTRIBUTION AMPLITUDES  
OF  $\eta$  AND  $\eta'$  MESONS**

**Shahin S. Agaev**

*Institute for Physical Problems  
Baku State University  
Z. Khalilov st. 23, Az-1148 Baku  
Azerbaijan*

The Partonic Structure of Hadrons  
ECT\* Trento  
May 9-14, 2005

## I. INTRODUCTION

Quark and gluon components of the  $\eta$  and  $\eta'$  mesons:

- 1)  $B \rightarrow K\eta'$  - and other exclusive B decays,  
 $B \rightarrow \eta'X$  - and other semi-inclusive B decays,
- 2) parameters of the  $\eta - \eta'$  mixing: mixing angles, decay constants,
- 3) distribution amplitudes of the  $\eta$  and  $\eta'$  mesons.

### Our approach:

- standard hard-scattering approach (Brodsky-Lepage factorization formula),
- methods of the infrared renormalon calculus (to evaluate power-suppressed corrections arising from the end-point integration regions ),
- $\eta\gamma$  and  $\eta'\gamma$  electromagnetic transition form factors: CLEO data to extract constraints on the parameters of the relevant DAs.

## II. $\eta - \eta'$ mixing schemes

- 1)  $SU_f(3)$  singlet-octet basis

$$|\eta_1\rangle = \frac{1}{\sqrt{3}} |u\bar{u} + d\bar{d} + s\bar{s}\rangle,$$

$$|\eta_8\rangle = \frac{1}{\sqrt{6}} |u\bar{u} + d\bar{d} - 2s\bar{s}\rangle.$$

Then the physical states take the form

$$|\eta\rangle = \cos\theta_p |\eta_8\rangle - \sin\theta_p |\eta_1\rangle,$$

$$|\eta'\rangle = \sin\theta_p |\eta_8\rangle + \cos\theta_p |\eta_1\rangle.$$

$\theta_p$  - mixing angle of physical states.

Decay constants  $f_8$ ,  $f_1$ ;

$$\langle 0 | J_\mu^{1(8)} | M \rangle = i f_M^{1(8)} p_\mu , \quad M \equiv \eta, \eta'$$

i) standard parametrization scheme; decay constants follow the pattern of the state mixing:

$$f_\eta^8 = f_8 \cos\theta_p , \quad f_\eta^1 = -f_1 \sin\theta_p ,$$

$$f_{\eta'}^8 = f_8 \sin\theta_p , \quad f_{\eta'}^1 = f_1 \cos\theta_p .$$

ii) two-angles mixing scheme

$$f_\eta^8 = f_8 \cos\theta_8 , \quad f_\eta^1 = -f_1 \sin\theta_1 ,$$

$$f_{\eta'}^8 = f_8 \sin\theta_8 , \quad f_{\eta'}^1 = -f_1 \cos\theta_1 ,$$

and

$$\theta_p \neq \theta_8 \neq \theta_1 .$$

The reasons to introduce two-angles mixing scheme: to explain experimental data within the standard HSA.

2)  $SU_f(3)$  quark-flavor basis

$$|\eta_q\rangle = \frac{1}{\sqrt{2}}|u\bar{u} + d\bar{d}\rangle,$$

$$|\eta_s\rangle = |s\bar{s}\rangle.$$

We use the singlet-octet basis and standard parametrization.

### III. $\eta\gamma$ and $\eta'\gamma$ transition form factors

In the framework of the  $SU_f(3)$  singlet-octet basis we have

$$F_{M\gamma}(Q^2) = F_{M\gamma}^1(Q^2) + F_{M\gamma}^8(Q^2),$$

where the singlet and octet components are given by:

$$Q^2 F_{M\gamma}^1(Q^2) = f_M^1 N_1 \left\{ T_{H,0}(x) \otimes \phi_1(x, \mu_F^2) \right.$$

$$+ \frac{\alpha_s(\mu_R^2)}{4\pi} C_F \left[ T_{H,1}(x, Q^2, \mu_F^2) \otimes \phi_1(x, \mu_F^2) \right.$$

$$\left. \left. + T_{H,1}^g(x, Q^2, \mu_F^2) \otimes \phi_1^g(x, \mu_F^2) \right] \right\},$$

$$Q^2 F_{M\gamma}^8(Q^2) = f_M^8 N_8 \left\{ T_{H,0}(x) \otimes \phi_8(x, \mu_F^2) \right.$$

$$+ \frac{\alpha_s(\mu_R^2)}{4\pi} C_F T_{H,1}(x, Q^2, \mu_F^2) \otimes \phi_8(x, \mu_F^2) \right\},$$

$T_{H,0}(x)$  - the leading order hard-scattering amplitude,

$T_{H,1}^{q(g)}(x, Q^2, \mu_F^2)$  - NLO hard-scattering amplitudes,

$N_1, N_8$  - numerical constants, each depending on the quark structure of the  $\eta_1, \eta_8$  states,

$\phi_1(x, \mu_F^2), \phi_1^g(x, \mu_F^2)$  - quark and gluon components of the DA of the  $\eta_1$  state,

$\phi_8(x, \mu_F^2)$  - DA of the  $\eta_8$  state (quark component only).

General form of DAs (for  $\eta_1$  state):

$$\phi^q(x, \mu_F^2) = 6x\bar{x} \left[ 1 + \sum_{n=2,4,\dots}^{\infty} \left\{ B_n^q \left[ \frac{\alpha_s(\mu_0^2)}{\alpha_s(\mu_F^2)} \right]^{\frac{\gamma_+^n}{\beta_0}} + \rho_n^g B_n^g \left[ \frac{\alpha_s(\mu_0^2)}{\alpha_s(\mu_F^2)} \right]^{\frac{\gamma_-^n}{\beta_0}} \right\} C_n^{3/2}(x - \bar{x}) \right],$$

$$\phi^g(x, \mu_F^2) = x\bar{x} \sum_{n=2,4,\dots}^{\infty} \left\{ \rho_n^q B_n^q \left[ \frac{\alpha_s(\mu_0^2)}{\alpha_s(\mu_F^2)} \right]^{\frac{\gamma_+^n}{\beta_0}} + B_n^g \left[ \frac{\alpha_s(\mu_0^2)}{\alpha_s(\mu_F^2)} \right]^{\frac{\gamma_-^n}{\beta_0}} \right\} C_{n-1}^{5/2}(x - \bar{x}).$$

We employ phenomenological DAs for the  $\eta_1, \eta_8$  states containing only first Gegenbauer polynomials:

$$\phi_1(x, \mu_F^2) = 6x\bar{x} [1 + A(\mu_F^2) - 5A(\mu_F^2)x\bar{x}],$$

$$\phi_1^g(x, \mu_F^2) = x\bar{x}(x - \bar{x})B(\mu_F^2),$$

and

$$\phi_8(x, \mu_F^2) = 6x\bar{x} [1 + C(\mu_F^2) - 5C(\mu_F^2)x\bar{x}] .$$

The functions  $A(\mu_F^2)$ ,  $B(\mu_F^2)$  and  $C(\mu_F^2)$  have the following forms ( $n_f = 3$ ):

$$A(\mu_F^2) = 6B_2^q(\mu_0^2) \left[ \frac{\alpha_s(\mu_F^2)}{\alpha_s(\mu_0^2)} \right]^{\frac{48}{81}} - \frac{B_2^g(\mu_0^2)}{15} \left[ \frac{\alpha_s(\mu_F^2)}{\alpha_s(\mu_0^2)} \right]^{\frac{101}{81}},$$

$$B(\mu_F^2) = 16B_2^q(\mu_0^2) \left[ \frac{\alpha_s(\mu_F^2)}{\alpha_s(\mu_0^2)} \right]^{\frac{48}{81}} + 5B_2^g(\mu_0^2) \left[ \frac{\alpha_s(\mu_F^2)}{\alpha_s(\mu_0^2)} \right]^{\frac{101}{81}},$$

$$C(\mu_F^2) = 6B_2^q(\mu_0^2) \left[ \frac{\alpha_s(\mu_F^2)}{\alpha_s(\mu_0^2)} \right]^{\frac{50}{81}}.$$

Our aim is extraction of the parameters:

$$B_2^q(\eta_1), \quad B_2^g(\eta_1) \quad \text{and} \quad B_2^q(\eta_8).$$

#### **IV. Choice of the renormalization scale $\mu_R^2$ and the running coupling (RC) method**

$\mu_R^2 = Q^2 x$  - quark virtuality in the leading order Feynman diagram (subprocess  $\gamma^* + \gamma \rightarrow q + \bar{q}$ )

In the second diagram the virtuality is equal to  $\bar{\mu}_R^2 = Q^2 \bar{x}$ , obtainable from  $\mu_R^2$  after  $x \leftrightarrow \bar{x}$  replacement (gauge invariant expres.).

$$Q^2 F_{M\gamma}^1(Q^2) = f_M^1 N_1 \{ T_{H,0}(x) \otimes \phi_1(x, \mu_F^2) \}$$

$$\begin{aligned} & + \frac{C_F}{2\pi} [\alpha_s(Q^2 x) t(x, \mu_F^2) \otimes \phi_1(x, \mu_F^2) \\ & + \alpha_s(Q^2 x) g(x, \mu_F^2) \otimes \phi_1^g(x, \mu_F^2)] \} \end{aligned}$$

$$Q^2 F_{M\gamma}^8(Q^2) = f_M^8 N_8 \{ T_{H,0}(x) \otimes \phi_8(x, \mu_F^2) \}$$

$$+ \frac{C_F}{2\pi} \alpha_s(Q^2 x) t(x, \mu_F^2) \otimes \phi_8(x, \mu_F^2) \}$$

Here  $t(x, \mu_F^2)$ ,  $g(x, \mu_F^2)$  are hard-scattering functions.

Singularities in the end-point region  $x \rightarrow 0$ .

Transformation:

$$\alpha_s(Q^2 x) = \frac{4\pi}{\beta_0} \int_0^\infty du \exp(-ut) x^{-u} R(u, t),$$

$$R(u, t) = 1 - \frac{2\beta_1}{\beta_0^2} u (1 - \gamma_E - \ln t - \ln u), \quad t = \ln(Q^2 / \Lambda^2).$$

Using this expression for  $\alpha_s(Q^2 x)$  one obtains the inverse Borel transformation for the form factors. For example:

$$\begin{aligned} Q^2 F_{M\gamma}^1(Q^2) &= f_M^1 N_1 \left( 6 + A(\mu_F^2) + \frac{12C_F}{\beta_0} \left\{ \left[ 1 + A(\mu_F^2) \right] \int_0^\infty du e^{-ut} R(u, t) Q_1(u) \right. \right. \\ &\quad \left. \left. - 5A(\mu_F^2) \int_0^\infty du e^{-ut} R(u, t) Q_2(u) \right\} + \frac{2C_F}{\beta_0} B(\mu_F^2) \int_0^\infty du e^{-ut} R(u, t) G(u) \right), \end{aligned}$$

with

$$Q_1(u) = \frac{2}{(1-u)^3} - \frac{2}{(2-u)^3} + \frac{1}{(1-u)^2} - \frac{9}{(1-u)(2-u)},$$

and similar formulas for  $Q_2(u)$  and  $G(u)$ . Inverse Borel transformation contains: finite number of triple, double and single poles.

Integrals: Cauchy principal value.

## V. Renormalons and power corrections.

$$\frac{4\pi}{\beta_0} \int_0^\infty \frac{\exp(-ut) du}{n-u} = \int_0^1 \alpha_s(Q^2 x) x^{n-1} dx = \frac{1}{n} f_{2n}(Q),$$

$f_p(Q)$  moment integrals. They can be written down in the form (Infrared matching scheme; B. Webber)

$$f_p(Q) = \left( \frac{\mu_I}{Q} \right)^p f_p(\mu_I) + \text{perturbative part}$$

$\mu_I$  - infrared matching scale,

$f_p(\mu_I)$  - new parameters (weighted averages of  $\alpha_s(k^2)$  over infrared region  $0 < k < \mu_I$ ).

### Asymptotic limit.

In the  $\lim Q^2 \rightarrow \infty$  we get

$$[Q^2 F_{M\gamma}(Q^2)]^{res} \rightarrow \frac{1}{\sqrt{3}} (4f_M^1 + \sqrt{2}f_M^8) \left[ 1 - \frac{5}{3\pi} \alpha_s(Q^2) \right].$$

## **VI. Numerical results**

We have used:

$$\Lambda(n_f = 4) = 0.25 \text{ GeV} , \mu_0^2 = 1 \text{ GeV}^2 , \mu_F^2 = Q^2$$

i) standard mixing scheme

$$f_1 = 1.17 f_\pi , f_8 = 1.26 f_\pi , \theta_p = -15.4^\circ ,$$

ii) two-mixing angles scheme

$$\theta_p = -15.4^\circ , \theta_1 = -9.2^\circ , \theta_8 = -21.2^\circ .$$

**Fig. 1.** Standard mixing scheme. HSA and RC methods.

Solid:  $B_2^q(\eta_1) = B_2^q(\eta_8) = 0, B_2^g = 0,$

Dashed:  $B_2^q(\eta_1) = B_2^q(\eta_8) = -0.05, B_2^g = 0,$

Dot-dashed:  $B_2^q(\eta_1) = B_2^q(\eta_8) = 0.1, B_2^g = 0,$

Short-dashed:  $B_2^q(\eta_1) = B_2^q(\eta_8) = 0, B_2^g = 15.$

**Fig. 2.** Standard mixing scheme. RC method.

Solid:  $B_2^g = 0,$

Dashed:  $B_2^g = 10,$

Dot-dashed:  $B_2^g = 15.$

**Fig. 3.** Standard mixing scheme. RC method.

$1\sigma$  regions. Central curves:  $B_2^q(\eta_1) = B_2^q(\eta_8) = 0.05, B_2^g = 17.$

**Fig. 4.**  $1\sigma$  region for DAs' parameters.

**Fig. 5.** Standard mixing scheme. RC method.

Solid:  $\theta_p = -15.4^\circ ,$

Dashed:  $\theta_p = -16.4^\circ ,$

Dot-dashed:  $\theta_p = -14.4^\circ .$

**Fig. 6.** Standard mixing scheme. RC method. The mixing angle is  $\theta_p = -15.4^\circ$ .

Solid:  $f_1/f_\pi = 1.17, f_8/f_\pi = 1.26,$

Dashed:  $f_1/f_\pi = 1.17, f_8/f_\pi = 1.30,$

Dot-dashed:  $f_1/f_\pi = 1.20, f_8/f_\pi = 1.28.$

**Fig. 7.** Standard and two-mixing angles schemes. RC method.

Solid (standard):  $B_2^q(\eta_1) = B_2^q(\eta_8) = 0.02, B_2^g = 18,$

Dashed: (2- mix. ang.):  $B_2^q(\eta_1) = B_2^q(\eta_8) = 0.02, B_2^g = 18,$

Dot-dashed(2-mix. ang.):  $B_2^q(\eta_1) = B_2^q(\eta_8) = 0.15, B_2^g = 18.$

**Fig. 8.** Standard mixing scheme and RC method.

Solid: standard prediction

Broken lines: standard  $\pm$  higher-twist uncertainties,

Dashed:  $N_q = 0.9, q = 1,2,3,4,$

Dot-dashed:  $N_q = -0.6.$

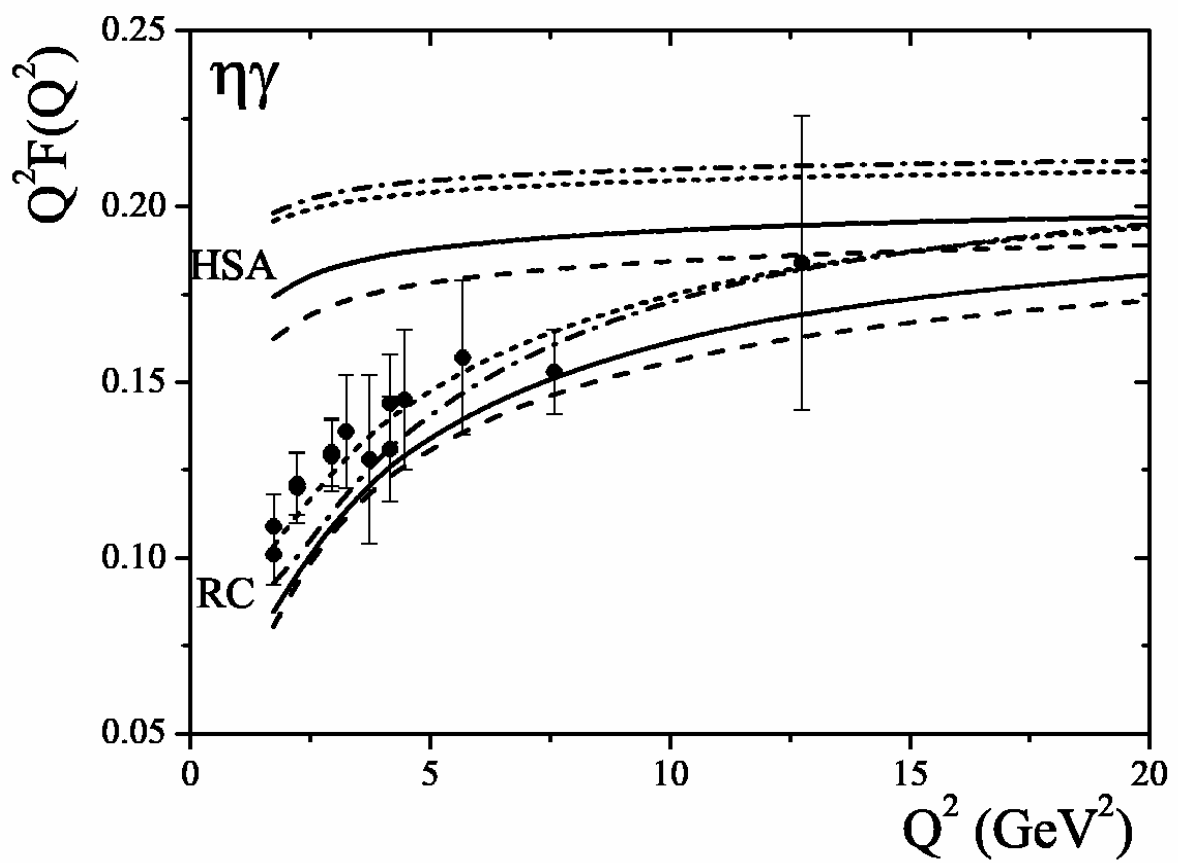


Fig. 1.

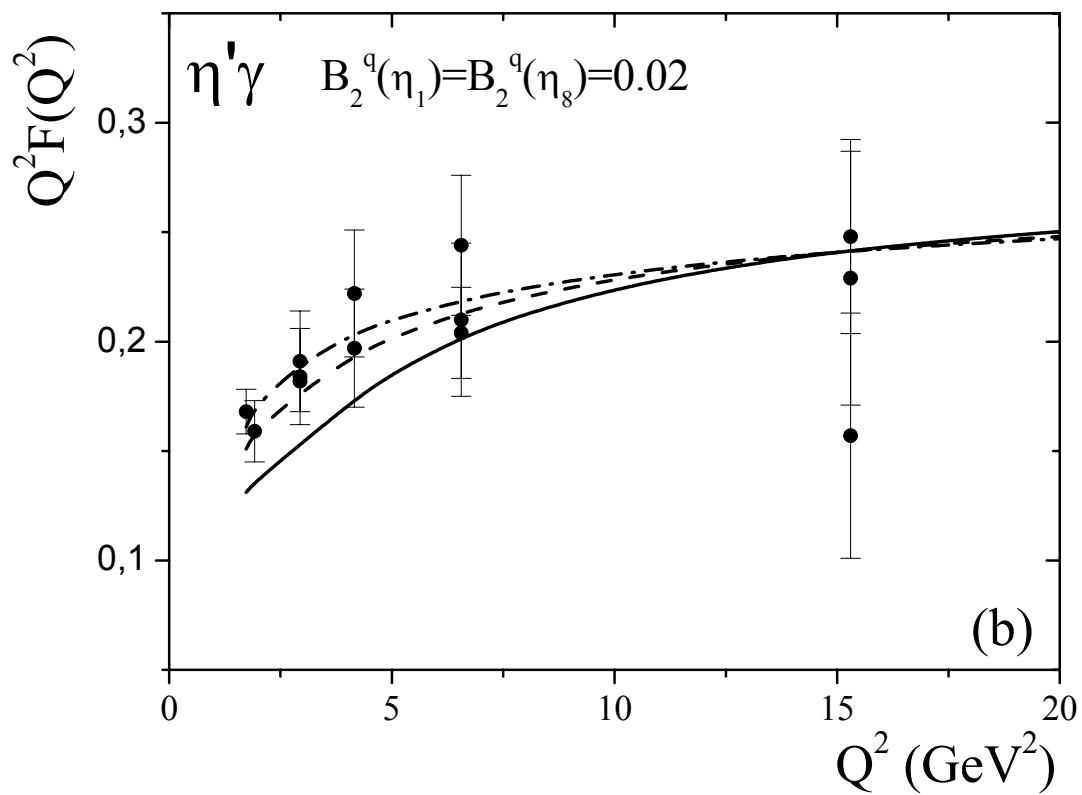
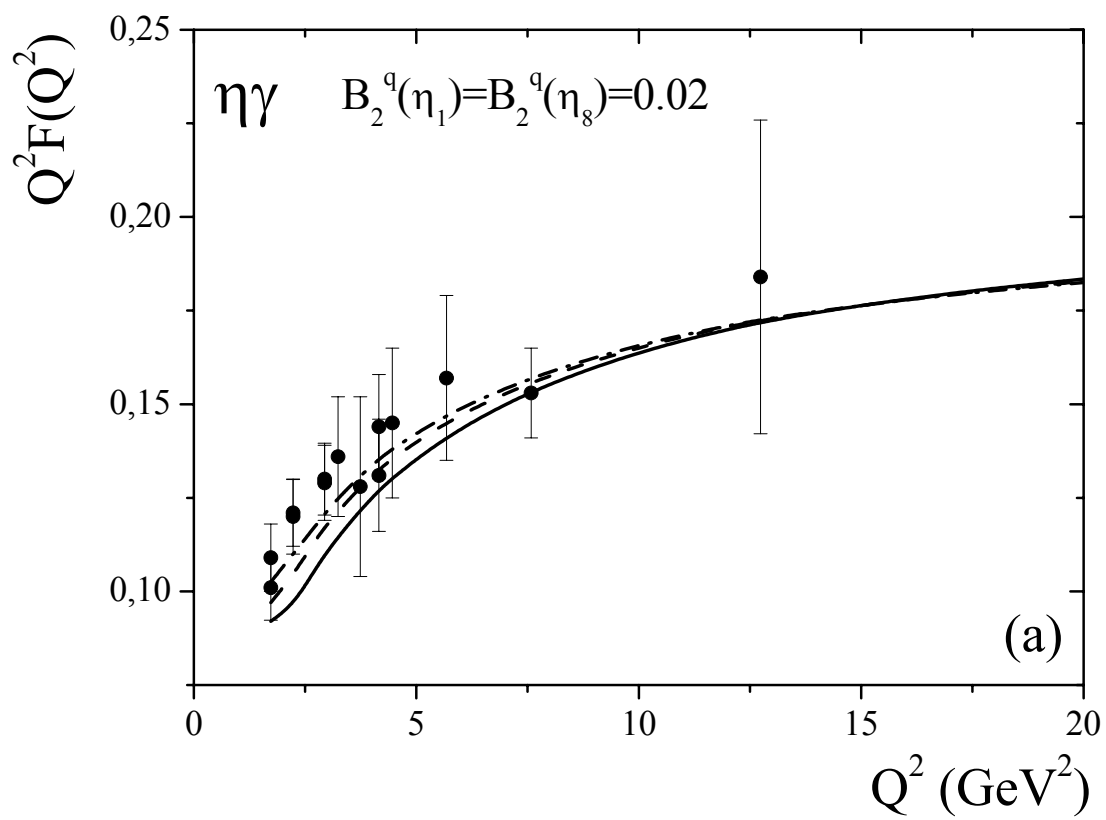


Fig. 2.

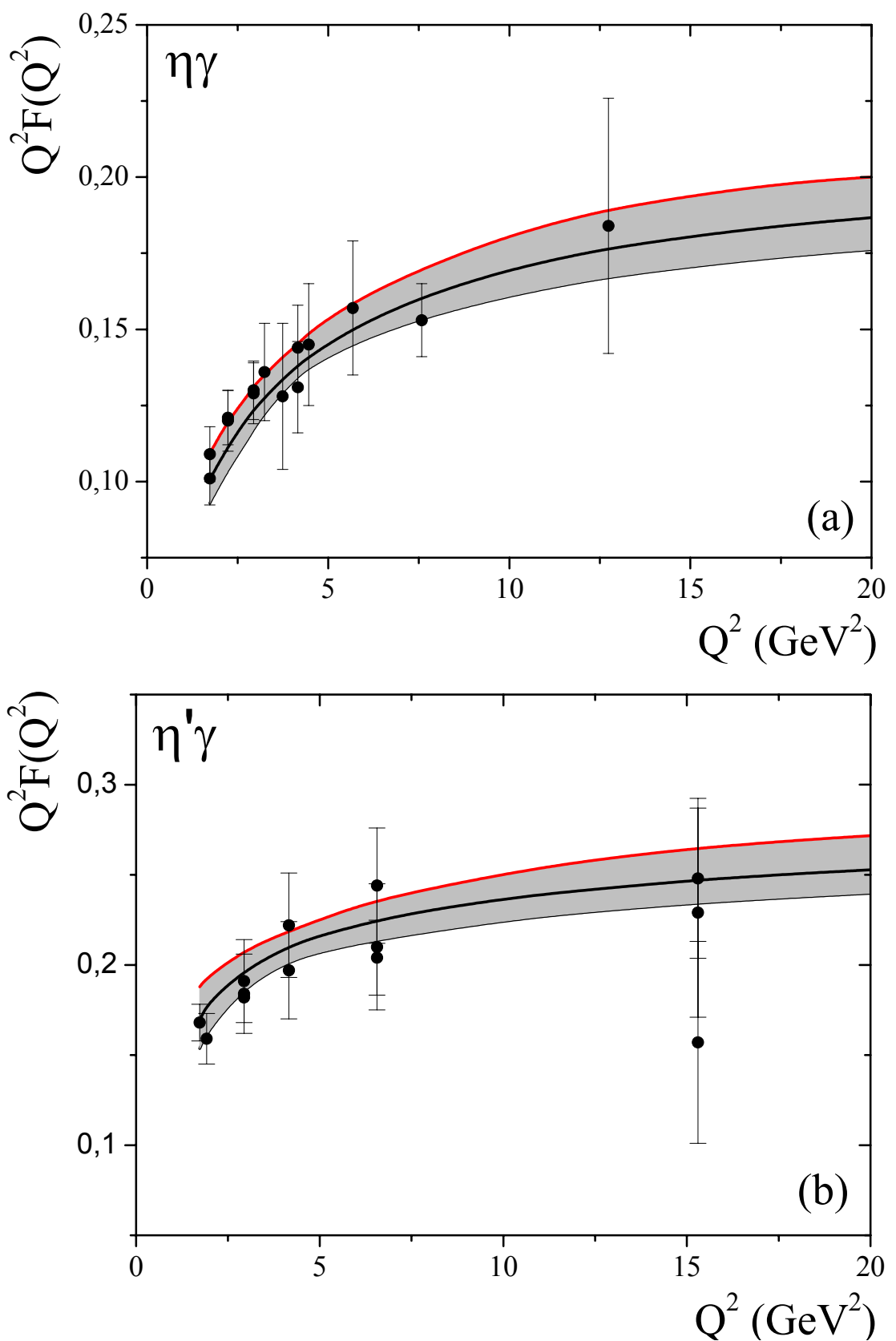


Fig. 3.

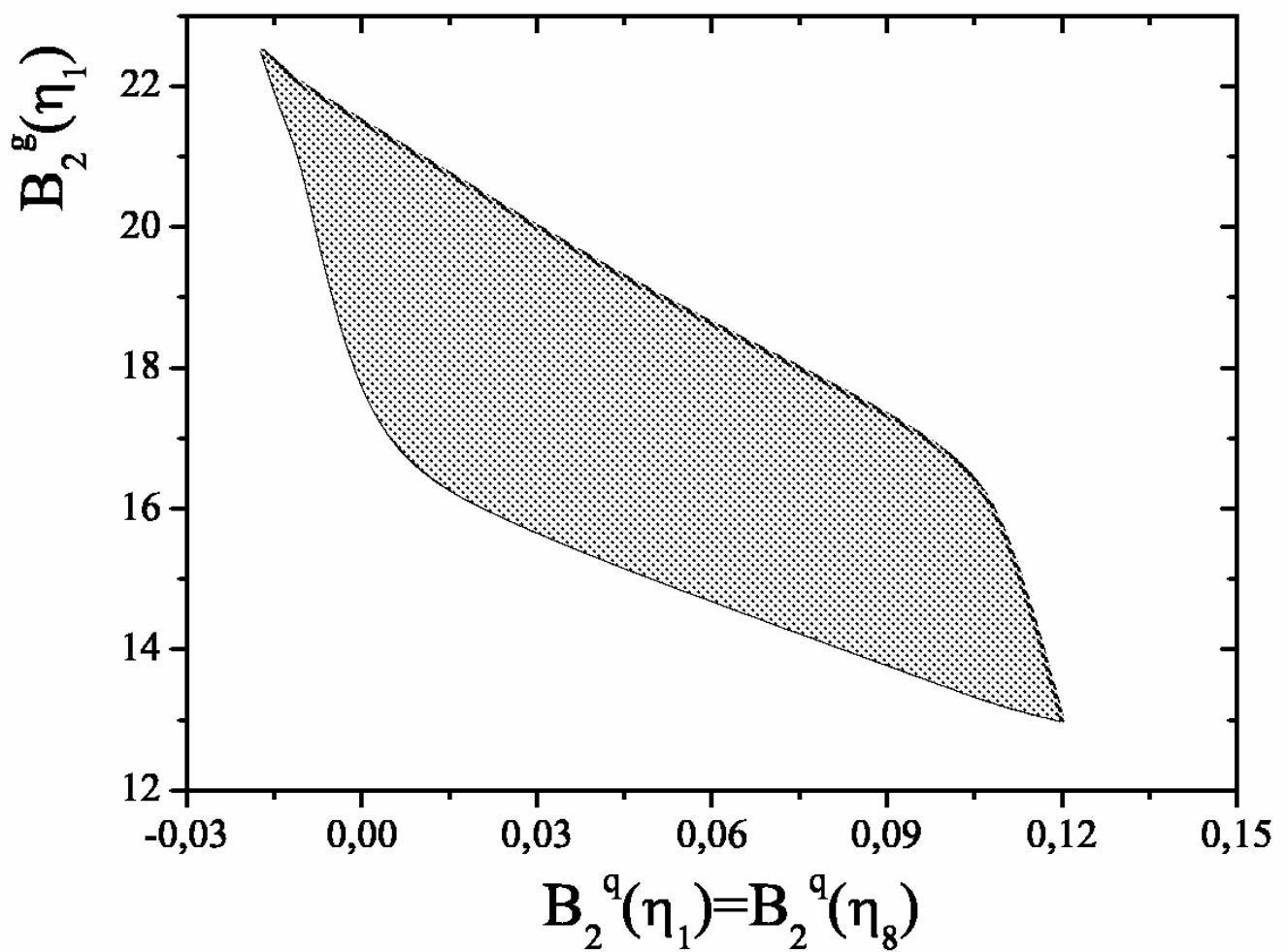
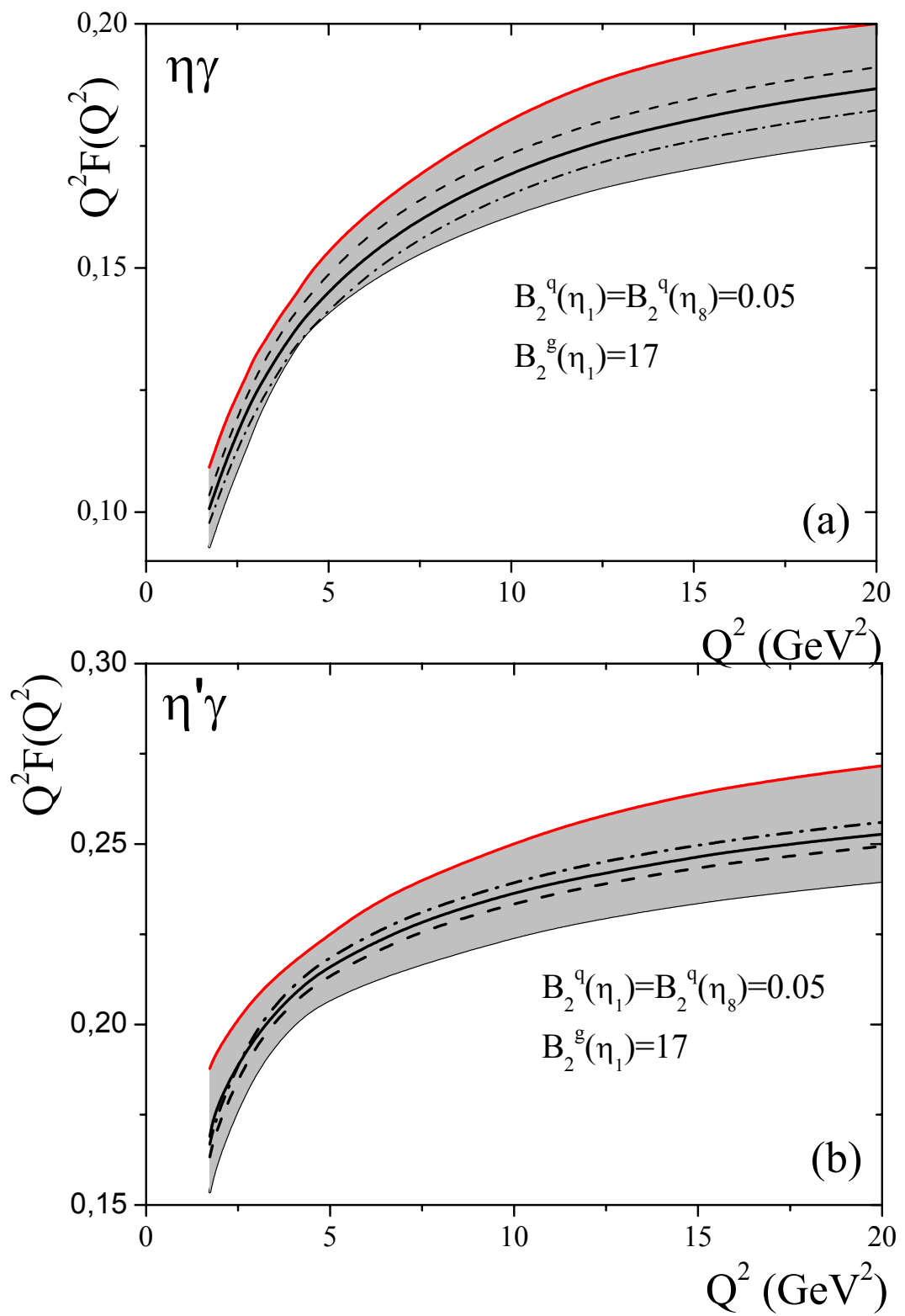


Fig. 4.

Fig. 5.



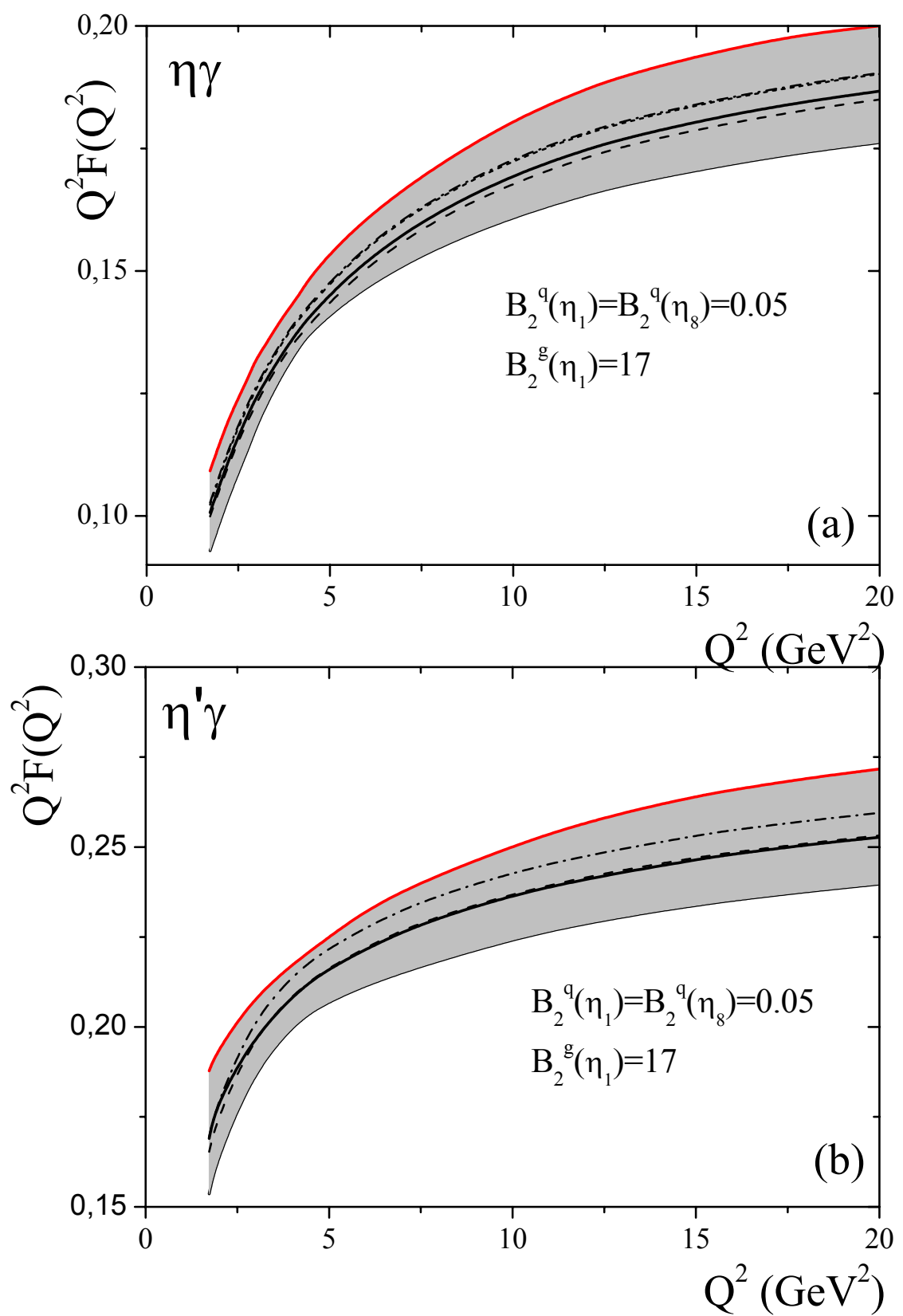


Fig. 6.

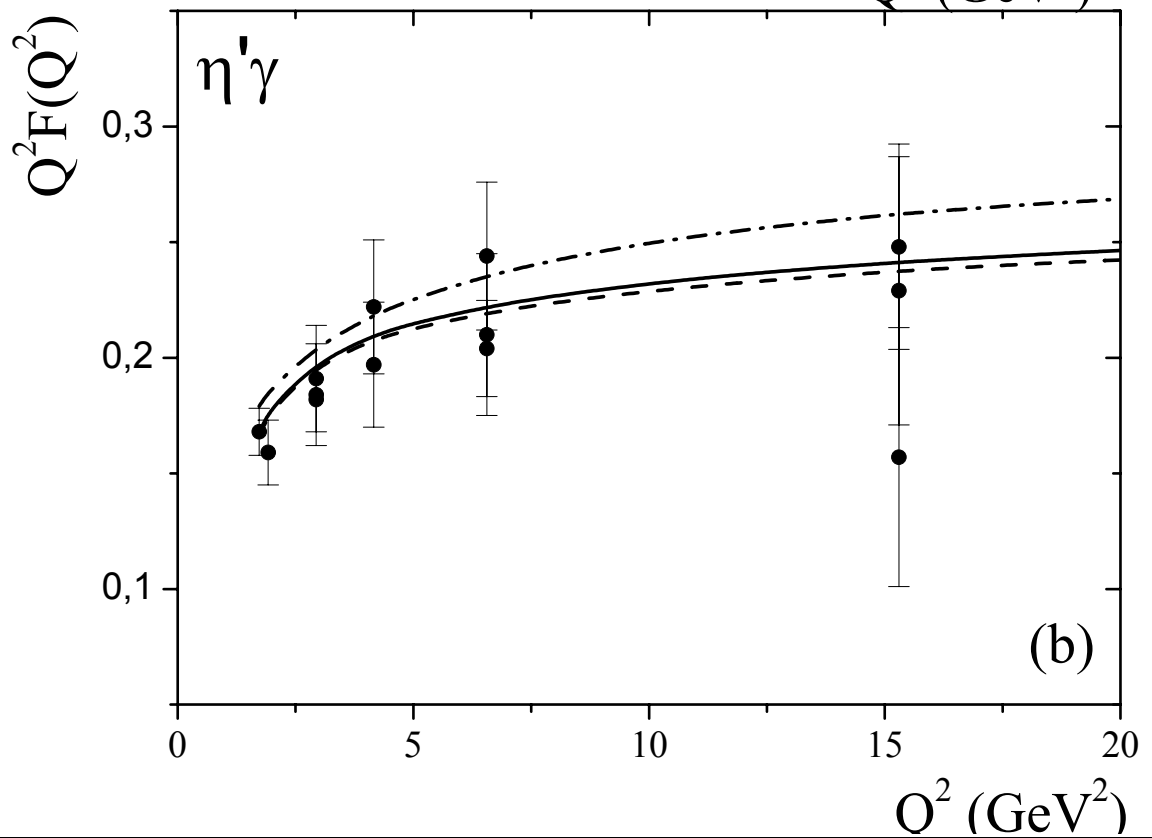
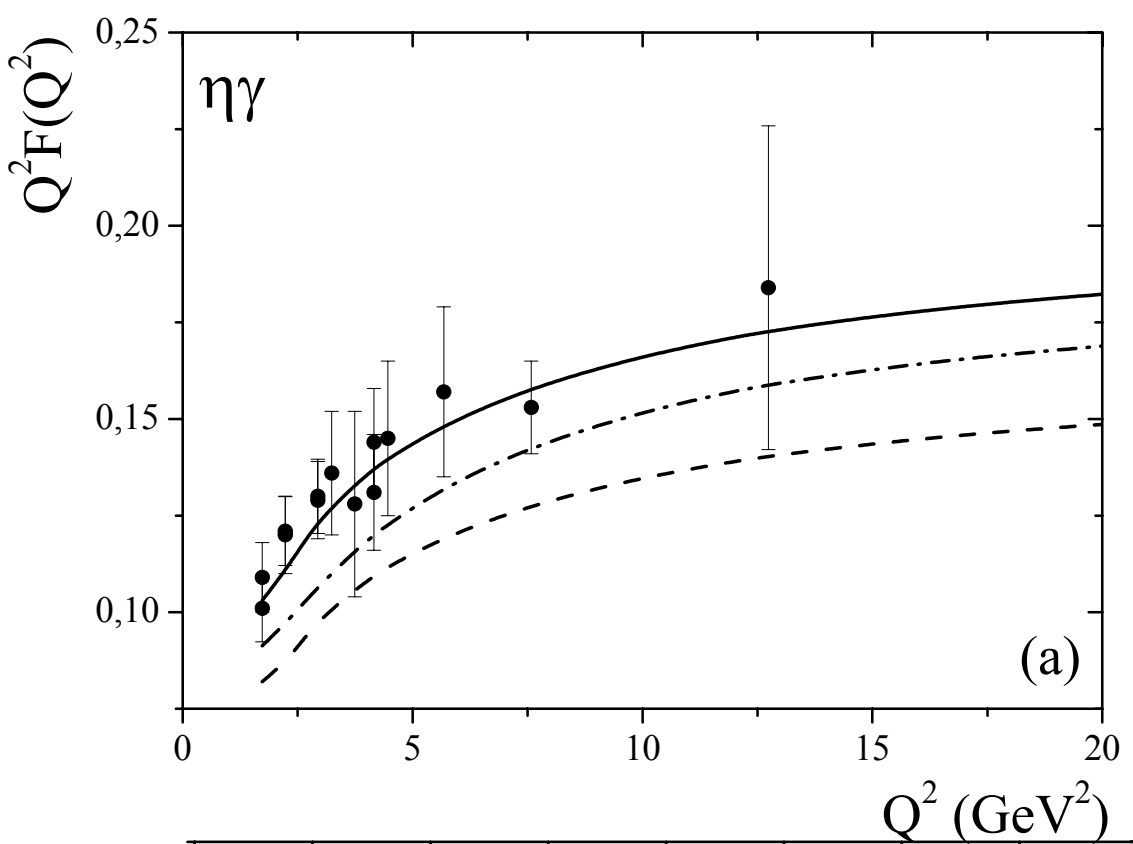


Fig. 7.

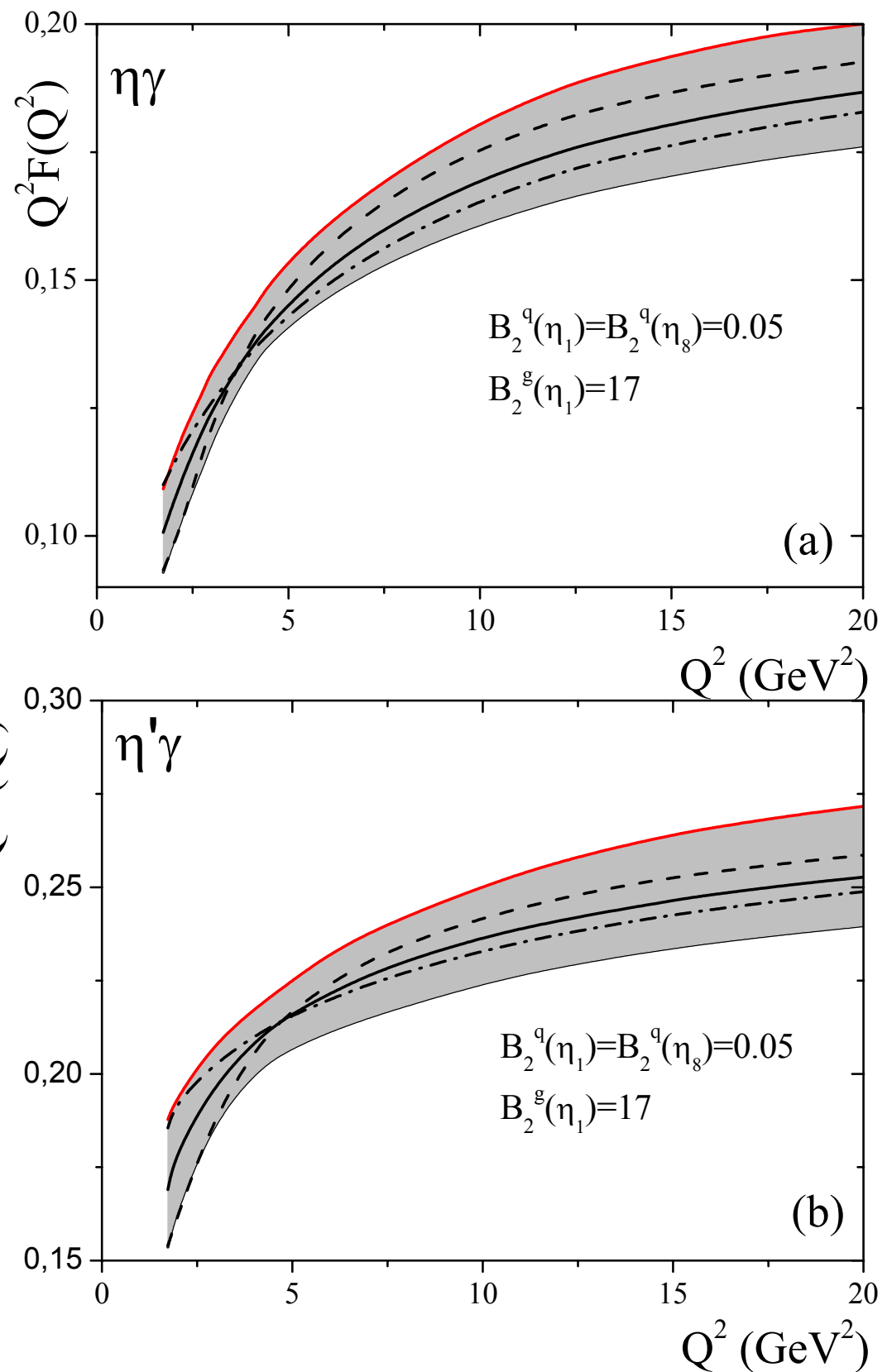


Fig. 8.

## **CONCLUSIONS:**

- i) power-suppressed corrections at moderate values of the momentum-transfers  $Q^2 \leq 5 \text{ GeV}^2$  enhance the absolute value of the  $O(\alpha_s)$  correction to the FFs approximately 2 times,
- ii) the gluonic contribution arising from the  $\eta_1$  DA [ $B_2^g > 0$ ] enhances the transition FFs in the region  $1.5 \text{ GeV}^2 \leq Q^2 \leq 12 \text{ GeV}^2$ . This effect is sizeable for the  $\eta'\gamma$  transition FF,
- iii) within the RC method the  $SU_f(3)$  singlet-octet basis and standard parametrization [ $\theta_p = \theta_1 = \theta_8$ ] of the decay constants  $f_1, f_8$  correctly describe the CLEO experimental data,
- iv) input parameters in DAs of the  $\eta_1$  and  $\eta_8$  states at the normalization point  $\mu_0^2 = 1 \text{ GeV}^2$  should obey:

$$B_2^q(\eta_1) = B_2^q(\eta_8) = 0.055 \pm 0.065,$$
$$B_2^g = 18 \mp 4.5.$$

- v) transition form factors (therefore, parameters in DAs) are stable against variation of the factorization scale  $Q^2/2 \leq \mu_F^2 \leq 2Q^2$ . The variation of the QCD parameter  $\Lambda$  modifies the  $1\sigma$  region shown in Fig. 4.

**Details can be found: S. S. Agaev, Phys. Rev. D64, 014007, 2001;  
S. S. Agaev and N. G. Stefanis, Phys. Rev. D70, 054020, 2004  
and hep-ph/0409198.**

